X-ray Data Collection, Structure Determination, and Refinement for $Cp_2Ti(PF_3)_2$ (3). Single crystals of the compound, grown by slow vacuum sublimation, were sealed in thin-walled glass capillaries prior to X-ray examination. Final lattice parameters as determined from a least-squares refinement of the angular settings of 15 reflections ($2\theta > 40°$) accurately centered on the diffractometer are given in Table III. Systematic absences allowed a space group choice of *C2cm*, *Cmc*2, and *Cmcm*. Successful solution and refinement of the structure indicated the correct choice to be the noncentrosymmetric *C2cm*.

Data were collected as described for the previous compound. The intensities were corrected for Lorentz and polarization effects, but not for absorption. Neutral-atom scattering factors were obtained as noted above, and that of titanium was corrected for the real and imaginary components of anomalous dispersion.

The positions of the two independent titanium atoms were revealed by the inspection of a Patterson map, and the subsequent calculation of a difference Fourier map allowed the location of the remaining non-hydrogen atoms. Refinement with isotropic thermal parameters led to a reliability index of $R = 0.081$. The hydrogen atoms of the cyclopentadienyl rings were placed at calculated positions 1.08 Å from the bonded carbon atom and were not refined. Refinement of the non-hydrogen atoms with anisotropic temperature factors led to final values of $R = 0.038$ and $R_w = 0.037$. A final difference Fourier showed no feature greater than 0.3 $e^-/Å^3$. The weighting scheme was based on unit weights; no systematic variation of $|F_o| - |F_c|$ vs. $|F_o|$ or $(\sin\theta)/\lambda$ was noted. The final values of the positional and thermal parameters are given in Tables VI and VII.[54]

(54) See paragraph at the end of paper regarding supplementary material.

Acknowledgment. We are grateful to the National Science Foundation (Grant CHE-8018210 to M.D.R. and Grant CHE-7809729 to J.L.A.) as well as the Exxon Research and Engineering Co. (grant to M.D.R.) for support of this research program. We also wish to thank G. Hlatky and Prof. J. Faller of Yale University for helpful discussions and assistance.

Supplementary Material Available: Tables of best planes results, and observed and calculated structure factor amplitudes (22 pages). Ordering information is given on any current masthead page.

Ab Initio Electronic Structures and Reactivities of Metal Carbene Complexes; Fischer-Type Compounds $(CO)_5Cr{=}CH(OH)$ and $(CO)_4Fe{=}CH(OH)$

H. Nakatsuji,* J. Ushio, S. Han,[1] and T. Yonezawa

Contribution from the Department of Hydrocarbon Chemistry, Faculty of Engineering, Kyoto University, Kyoto, Japan. *Received May 19, 1982*

Abstract: Electronic structures and reactivities of the chromium and iron carbene complexes $(CO)_5Cr{=}CH(OH)$ and $(CO)_4Fe{=}CH(OH)$ are studied by the ab initio SCF MO method, and the nature of the double bond between the metal and carbene carbon atom, $M{=}C_{carb}$, is investigated. The equilibrium $M{=}C_{carb}$ length is calculated to be 2.00 Å for both Cr and Fe carbene complexes, in reasonable agreement with the experimental value 2.04 Å. The $M{=}C_{carb}$ bond energy is calculated to be 44.4 kcal/mol and 36.8 kcal/mol for the Cr and Fe carbenes, respectively. For the Fe carbene, the axial isomer is calculated to be more stable than the equatorial isomer by 8.1 kcal/mol. The barrier to rotation around the $M{=}C_{carb}$ bond is calculated to be very small (0.41 kcal/mol for $Cr{=}C_{carb}$ and 2.9 kcal/mol for $Fe{=}C_{carb}$), showing that the rotation is essentially free. This is in contrast to a large barrier of the C=C double bond in ethylene. The origins of the $M{=}C_{carb}$ double bond and of the smallness of the rotational barriers are clarified from the diagram of orbital correlation with the fragment orbitals. The differences in the natures of the $M{-}C_{carb}$ and M–CO bonds are clarified. The polarization of charge of the $M{=}C_{carb}$ bond is calculated to be $M^{\delta+}{-}C_{carb}^{\delta-}$ for both the Cr and Fe carbenes: the carbene carbon is calculated to be negatively charged in contradiction with the commonly accepted idea, though the electron is deficient in the π region of the carbene carbon atom. The electrophilic reactivity of the carbene carbon is not charge controlled, but is controlled by the frontier orbital, LUMO.

Metal carbene complexes, first synthesized by Fischer and co-workers,[2] are of remarkable importance as intermediates of many organometallic reactions[2-4] such as olefin metathesis[5] catalytic reduction of CO by H_2,[6] Ziegler–Natta polymerization reaction,[5,7] etc. The nature of the metal–carbon double bond involved is also of special interest as one of the typical bonding modes in organometallic chemistry. The varieties of geometries and spectroscopic properties are also of interest. In this series of papers, we study electronic structures and reactivities of metal carbene complexes. We are interested in the nature of the $M{=}C_{carb}$ bond, the origin of the reactivity of the carbene complexes, and their differences due to the difference in metal species. We report here the results of ab initio SCF MO calculations on the chromium and iron carbene complexes, $(CO)_5Cr{=}CH(OH)$ and

(1) On leave from the Department of Chemistry, Beijing Normal University, Beijing, China.

(2) Fischer, E. O.; Maasböl, A. *Angew. Chem.* **1964**, *76*, 645; *Angew. Chem., Int. Ed. Engl.* **1964**, *3*, 580. Fischer, E. O. *Adv. Organomet. Chem.* **1976**, *14*, 1.

(3) Cardin, D. J.; Cetinkaya, B.; Lappert, M. F. *Chem. Rev.* **1972**, *72*, 545.

(4) Cotton, F. A.; Wilkinson, G. "Advanced Inorganic Chemistry", 4th ed.; Wiley: New York, 1980.

(5) For example: Calderon, N.; Lawrence, J. P.; Ofstead, E. A. *Adv. Organomet. Chem.* **1979**, *17*, 449.

(6) For example: Vannice, M. A. *Catal. Rev.-Sci. Eng.* **1976**, *14*, 153.

(7) Ziegler, K.; Holzkamp, E.; Breil, H.; Martin, H. *Angew. Chem.* **1955**, *67*, 541. Natta, G. *Macromol. Chem.* **1955**, *16*, 213.

0002-7863/83/1505-0426$01.50/0

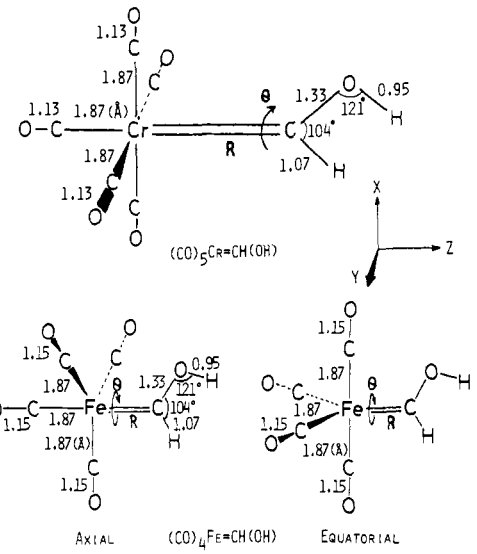

Figure 1. Geometries of the chromium and iron carbene complexes used in the present calculations.

$(CO)_4Fe{=}CH(OH)$, both Fischer-type compounds.

A previous sophisticated ab initio calculation on metal carbene complex is only for $(CO)_3NiCH_2$ by Spangler et al.[8] They examined the geometrical parameters of this complex and obtained the $Ni{=}C_{carb}$ distance of 1.83 Å, a bit shorter than the corresponding experimental distance of 1.909 Å. They also found that the rotational barrier around the $Ni{=}C_{carb}$ bond is as small as 0.16 kcal/mol. Block, Fenske, and Casey[9] reported MO calculations on $(CO)_5CrC(OCH_3)CH_3$ and $(CO)_5MnCOCH_3$, though their "nonempirical" method[10] is very much approximate. They concluded that the reactions of these complexes are frontier, rather than charge, controlled. Kostič and Fenske[11] also reported an MO calculation on carbyne complexes[2] by the same approximate method.

Here, we report the results of ab initio SCF MO calculations of the chromium and iron carbene complexes $(CO)_5Cr{=}CH(OH)$ and $(CO)_4Fe{=}CH(OH)$. In the next section we summarize the calculational details. The method of calculations, the basis set used, the geometries of the complexes and their fragments, etc. are summarized. We then show the calculated results. We discuss the rotational barrier, stability, and other properties of the metal–carbon double bond. The equilibrium length, force constant, and heat of dissociation of the bond are calculated. For the Fe complex, the stable conformation, axial or equatorial, is examined. The nature and the electronic origin of the $M{=}C_{carb}$ bonds are further clarified on the basis of the diagram of orbital correlation with the fragment orbitals. We will then show the charge distribution in the metal carbene complexes and analyze the extent of σ transfer and π back-transfer. We compare the interaction in the $M{-}C_{carb}$ bond with that of the M–CO bond. We will point out a contradiction of the present result with the commonly accepted idea on the charge distribution and show a resolution. The reactivity of the metal carbene complex is explained as frontier orbital controlled rather than charge controlled. The conclusions of the present study are summarized in the last section.

Calculational Details

We have carried out ab initio SCF MO calculations based on the closed-shell Hartree–Fock–Roothaan theory.[12] We have used a slightly modified version of the HONDOG program due originally to King, Dupuis, and Rys.[13] The basis sets for Cr and Fe are the MINI-2 basis set due

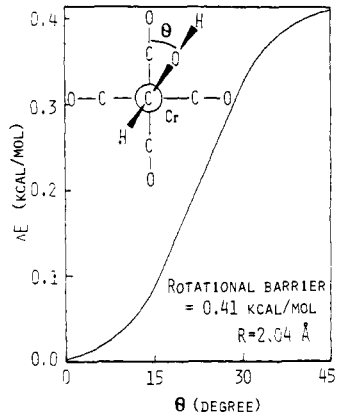

Figure 2. Potential curve for the rotation around the $Cr{=}C_{carb}$ bond of $(CO)_5Cr{=}CH(OH)$.

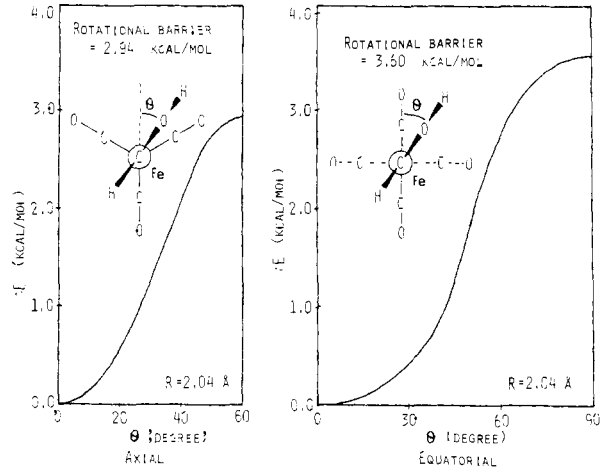

Figure 3. Potential curves for the rotation around the $Fe{=}C_{carb}$ bonds in the axial and equatorial isomers of $(CO)_4Fe{=}CH(OH)$.

to Tatewaki and Huzinaga[14] supplemented by the 4p AO with the exponent same as that for the 4s AO. For C, O, and H atoms, we have used minimal 3G CGTO by Tavouktsoglou and Huzinaga.[15]

The geometries of the metal carbene complexes used in the present calculations are shown in Figure 1. For $(CO)_5CrCH(OH)$, we have referred to the geometry of the similar compound, $(CO)_5CrC(OMe)Ph$, reported by Mills and Redhouse.[16] The Cr–CO(trans) distance, 1.87 Å, is also used for Cr–CO(cis). The carbene fragment, CH(OH), was kept planar and the two protons were put cis to each other. The CH and OH distances were cited from similar compounds.[17] Since we are interested in the nature of the $Cr{=}C_{carb}$ bond, we have investigated the changes in the electronic structure and the potential energy along with the change in the $Cr{=}C_{carb}$ distance, R, and with the rotation around the $Cr{=}C_{carb}$ bond, θ.

For $(CO)_4FeCH(OH)$, we have considered two geometrical isomers, axial and equatorial isomers, in which the carbene ligands are at the axial and equatorial positions, respectively. Because of the lack of the experimental geometry, we have used the geometry of the related compounds. For the $(CO)_4Fe$ fragments, we have referred to the geometry of $Fe(CO)_5$.[17] The geometrical parameters for axial and equatorial CO's were set equal. The geometry of the CH(OH) fragment is equal to that in the Cr carbene. Since we are interested in the nature of the $Fe{=}C_{carb}$ bond, we have varied the $Fe{=}C_{carb}$ distance R and the rotational angle θ around the $Fe{=}C_{carb}$ bond.

We have also studied the electronic structures of the isolated fragments, $(CO)_5Cr$, $(CO)_4Fe$, and CH(OH). The geometries of the fragments were taken equal to those of the carbene complexes. For $(CO)_4Fe$, both axial and equatorial isomers were calculated.

The metal carbene complexes are considered as products of the combination reaction of the above fragments. The spin states of the frag-

(8) Spangler, D.; Wendoloski, J. W.; Dupuis, M.; Chen, M. M. L.; Schaefer, H. F., III. *J. Am. Chem. Soc.* **1981**, *103*, 3985.
(9) Block, T. F.; Fenske, R. F.; Casey, C. P. *J. Am. Chem. Soc.* **1976**, *98*, 441.
(10) Hall, M. B.; Fenske, R. F. *Inorg. Chem.* **1972**, *11*, 768.
(11) Kostič, N. M.; Fenske, R. F. *J. Am. Chem. Soc.* **1981**, *103*, 4677.
(12) Roothaan, C. C. J. *Rev. Mod. Phys.* **1951**, *23*, 69.
(13) King, H. F.; Dupuis, M.; Rys, J. Program Library HONDOG (No. 343) of the computer center of the Institute for Molecular Science, 1979.
(14) Tatewaki, H.; Huzinaga, S. *J. Chem. Phys.* **1979**, *71*, 4339.
(15) Tavouktsoglou, A. N.; Huzinaga, S. *J. Chem. Phys.* **1980**, *72*, 1385.
(16) Mills, O. S.; Redhouse, A. D. *J. Chem. Soc. A* **1968**, 642.
(17) Sutton, L. E. *Spec. Publ.-Chem. Soc.* **1958**, *No. 11*; **1965**, *No. 18*.

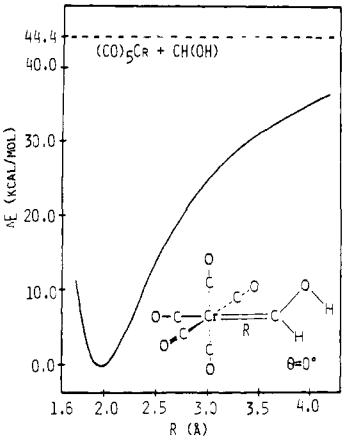

Figure 4. Potential curve for the singlet dissociation of the $Cr{=}C_{carb}$ bond of $(CO)_5Cr{=}CH(OH)$.

Table I. SCF Energies of $(CO)_5Cr{=}CH(OH)$ and $(CO)_4Fe{=}CH(OH)$ and Their Singlet and Triplet Fragments

molecule	total energy, au[a]
$(CO)_5Cr{=}CH(OH)$ (R = 2.04 Å, θ = 0°)	−1711.39408
$(CO)_5Cr$ fragment singlet	−1598.36782
triplet	−1598.35766
$(CO)_4Fe{=}CH(OH)$ (R = 2.04 Å, θ = 0°)	
axial	−1817.69830
equatorial	−1817.68545
$(CO)_4Fe$ fragment singlet	
axial	−1704.66512
equatorial	−1704.68448
CH(OH) fragment singlet	−112.95535
triplet	−112.93109

[a] 1 au = 627.504 kcal/mol.

ments can be both singlet or both triplet. We have calculated both of these spin states for the fragments of the Cr carbene. The singlet fragments were calculated by the closed-shell RHF method and the triplet fragments by the open-shell RHF method.[18] Though the Jahn–Teller distortion is expected for the triplet fragments, $(CO)_5Cr$ and axial $(CO)_4Fe$, we did not consider such effect, taking average distributions over degenerate orbitals in the SCF process.

Rotational Barrier around the Metal–Carbon (Carbene) Bond

We first show the potential curves for the rotation around the metal–carbon (carbene) bond. Figures 2 and 3 are for the chromium and iron carbenes, respectively, obtained with fixing the $M{=}C_{carb}$ distance at 2.04 Å. The calculated rotational barriers are as small as 0.41 kcal/mol for the chromium carbene and 2.94 and 3.60 kcal/mol for the axial and equatorial iron carbenes, respectively. The stable conformations are eclipsed in $(CO)_5Cr{=}CH(OH)$ between the cis CO and the plane of the carbene fragment, eclipsed in the equatorial $(CO)_4Fe{=}CH(OH)$ between the axial CO and the carbene plane, and staggered in the axial $(CO)_4Fe{=}CH(OH)$ between the CO and the C(OH) bond. The rotation around the $M{=}C_{carb}$ bond is essentially free, and this might be unexpected from the nature of double bonds in organic molecules; the rotational barrier in ethylene is, for example, 65 kcal/mol.[19] The calculated barriers are of the order of those around the C–C single bonds. In ethane it is 2.9 kcal/mol.[20] Spangler et al.[8] also reported, from ab initio calculations, the rotational barrier in $(CO)_3Ni{=}CH_2$ as small as 0.16 kcal/mol. The staggered conformation observed experimentally for $(CO)_5Cr{=}C(OMe)Ph$[16] is expected to be due to the bulky groups present in the carbene fragment or to the effects of intermolecular interactions in the crystal. From the considerations shown below based on the orbital correlation diagram, we believe that such

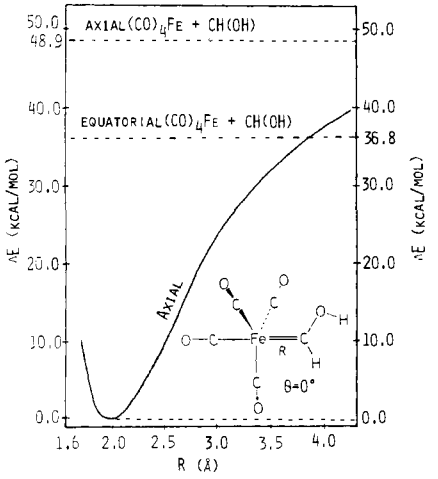

Figure 5. Potential curve for the singlet dissociation of the $Fe{=}C_{carb}$ bond of $(CO)_4Fe{=}CH(OH)$.

Table II. Stabilities and Properties of the $M{=}C_{carb}$ Bonds in Chromium and Iron Carbene Complexes

properties	$(CO)_5Cr{=}CH(OH)$	$(CO)_4Fe{=}CH(OH)$ axial[a]	$(CO)_4Fe{=}CH(OH)$ equatorial[a]
rotational barrier around $M{=}C_{carb}$ bond, kcal/mol	0.41	2.94	3.60
$M{=}C_{carb}$ bond energy, kcal/mol	44.4	36.8[b] (48.9)[c]	26.1
$M{=}C_{carb}$ length, Å	2.00[d]	2.00	1.96
force constant k, mdyn/Å	1.62	1.25	1.41
ω, cm^{-1} [e,f]	330–530	290–460	310–490

[a] Axial isomer is calculated to be more stable than the equatorial isomer by 8.1 kcal/mol. [b] Dissociation energy to equatorial $(CO)_4Fe$ and CH(OH) fragments. [c] Dissociation energy to axial $(CO)_4Fe$ and CH(OH) fragments. [d] The experimental $Cr{=}C_{carb}$ distance in $(CO)_5Cr{=}C(OMe)Ph$ is 2.04 Å (ref 16). [e] The vibrational frequency was calculated from the force constant in two approximations; the atoms and groups of atoms bonded to the metal and C_{carb} atoms are considered to completely follow or not to follow the vibration. The former approximation gives a minimum value and the latter a maximum one. [f] Experimental vibrational frequencies (M–C(O)) in $Cr(CO)_6$ and $Fe(CO)_5$ are 391–449 and 377–474 cm^{-1}, respectively (ref 28).

smallness of the rotational barrier around the $M{=}C_{carb}$ bond is generally valid for the Fischer type carbene complexes. Cardin et al.[3] expressed a similar opinion from experimental bases.

Stabilities and Properties of the Metal–Carbon (Carbene) Bonds

Figures 4 and 5 show the potential curves for the singlet dissociations of the $M{=}C_{carb}$ bonds of the chromium and iron carbene complexes, respectively. Table I shows the SCF energies of these complexes and their singlet and triplet fragments. Table II shows a summary of the theoretical results for the stabilities and the properties of the $M{=}C_{carb}$ bonds in chromium and iron carbene complexes.

From the SCF energies shown in Table I, the bond dissociation energy of the $Cr{=}C_{carb}$ bond of $(CO)_5Cr{=}CH(OH)$ to the singlet fragments $(CO)_5Cr$ and CH(OH) is calculated to be 44.4 kcal/mol. The potential curve of the bond dissociation shown in Figure 4 converges monotonously to the sum of the energies of these singlet fragments. This shows that the dissociation of the $Cr{-}C_{carb}$ bond leads to the ground states of the singlet fragments.

The dissociation to the triplet fragments may also be interested in, since the singlet–triplet energy separation of the carbene fragment is small. For the methylene CH_2, it is well-known that the triplet state is more stable than the singlet state by about 9 kcal/mol.[21,22] For CH(OH), however, the singlet state is more

(18) Roothaan C. C. J. *Rev. Mod. Phys.* **1960**, *32*, 179.
(19) Douglas, J. E.; Rabinovitch, B. S.; Looney, F. S. *J. Chem. Phys.* **1955**, *23*, 315.
(20) Lowe, J. P. *Prog. Phys. Org. Chem.* **1968**, *6*, 1.
(21) Simons, J. W.; Curry, R. *Chem. Phys. Lett.* **1976**, *38*, 171.

Table III. Orbital Energies and Coefficients of Some Important MO's of $(CO)_5Cr{=}CH(OH)$ and the Singlet Fragments $(CO)_5Cr$ and $CH(OH)^a$

		$(CO)_5Cr{=}CH(OH)$			$(CO)_5Cr$			CH(OH)	
		σ bonding MO	HOMO (π)	LUMO (π)	degenerate next HOMO	HOMO (δ)	LUMO (nσ)	HOMO (nσ)	LUMO (π)
ϵ_i, eV		−10.870	−6.335	3.858	−7.534	−6.909	1.731	−8.789	5.747
Cr	$3d_{x^2}$	−0.03	0.0	0.0	0.0	0.0	−0.15		
	d_{y^2}	−0.05	0.0	0.0	0.0	0.0	−0.15		
	d_{z^2}	0.19	0.0	0.0	0.0	0.0	0.15		
	d_{xy}	0.0	−0.03	0.01	0.0	0.75	0.0		
	d_{xz}	0.03	0.0	0.0	−0.02	0.0	0.0		
	d_{yz}	0.0	0.75	−0.16	0.86	0.0	0.0		
	4s	−0.02	0.0	0.0	0.0	0.0	0.41		
	p_x	−0.02	0.0	0.0	0.0	0.0	0.0		
	p_y	0.0	0.02	0.61	0.01	0.0	0.0		
	p_z	0.03	0.0	0.0	0.0	0.0	0.77		
C(carbene)	2s	0.46	0.0	0.0				0.58	0.0
	p_x	0.21	0.0	0.0				0.17	0.0
	p_y	0.0	0.22	0.66				0.0	0.97
	p_z	−0.64	0.0	0.0				−0.71	0.0
C(axial)	2s	−0.10	0.0	0.0	0.0	0.0	0.27		
	p_x	0.0	0.0	0.0	0.0	0.0	0.0		
	p_y	0.0	−0.16	0.25	0.14	0.0	0.0		
	p_z	−0.08	0.0	0.0	0.0	0.0	0.01		
C(equatorial)	2s	−0.05	0.0	0.0	0.0	0.0	−0.12		
	p_x	0.04	0.0	0.0	0.0	0.0	0.05		
	p_y	0.0	−0.01	0.10	0.01	0.17	0.0		
	p_z	0.0	0.0	0.0	0.10	0.0	0.14		

[a] See Figure 1 for the coordinates.

stable than the triplet state by the present theoretical value, 15.22 kcal/mol (without considering the change in geometry). For the $(CO)_5Cr$ fragment, the singlet state is calculated to be more stable than the triplet state by 6.38 kcal/mol. Thus, the dissociation energy of $(CO)_5CrCH(OH)$ into triplet fragments is calculated to be 66.1 kcal/mol. The triplet fragmentation requires more energy than the singlet fragmentation by 22.1 kcal/mol. Further, this theoretical value should be an underestimate, since the correlation energy (difference between the exact energy and the Hartree–Fock energy) should be larger for closed-shell singlet states than for open-shell triplet states. For CH_2, the effect of electron correlation on the singlet–triplet separation is ~17 kcal/mol.[23] A similar order of magnitude of the correlation correction is also expected for CH(OH) and $(CO)_5Cr$.

For the Fe carbene $(CO)_4Fe{=}CH(OH)$, two different conformations, axial and equatorial, are considered. In the present calculation the axial isomer is calculated to be more stable than the equatorial isomer by 8.1 kcal/mol. In the singlet dissociation limit, however, the equatorial fragment is calculated to be more stable than the axial one by 12.1 kcal/mol. Though the potential curve for the axial isomer shown in Figure 5 was obtained with keeping the $(CO)_4Fe$ fragment always axial, the more realistic potential curve would be for the process in which the $(CO)_4Fe$ fragment rearranges itself gradually from axial to equatorial conformation in the course of the dissociation. The dissociation energy of axial isomer with fixed conformation is calculated to be 48.9 kcal/mol and that with changing conformation to be 36.8 kcal/mol. The dissociation energy of the equatorial isomer is calculated to be 26.1 kcal/mol.

The bond energy of the C=C double bond in ethylene is 120 kcal/mol.[24] Though the bond energies of the metal carbon double bonds obtained here (44.4 kcal/mol for $Cr{=}C_{carb}$ and 36.8 kcal/mol for $Fe{=}C_{carb}$) are much smaller than this value, they still show a considerable stability of the $M{=}C_{carb}$ bond.

It is interesting to note that the stable geometries of the olefin coordinated iron complexes are equatorial rather than axial.[25] For example the geometry of (η^2-ethylene)tetracarbonyliron $Fe(CO)_4C_2H_4$ is reported as[26]

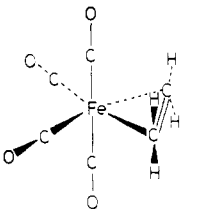

This is different from the present result for the iron carbene complex for which the axial isomer is more stable than the equatorial one. This difference is presumably due to the difference in the interaction strength between Fe and ligand. The coordination energy of olefin seems to be smaller than that of the carbene[27] and when the interaction is weak the stable geometry of the complex would be mainly determined by that of the $(CO)_4Fe$ fragment, i.e., equatorial.

The equilibrium bond length of the $M{=}C_{carb}$ double bond in $(CO)_5Cr{=}CH(OH)$ is calculated to be 2.00 Å, in good correspondence with 2.04 Å observed for $(CO)_5CrC(OMe)Ph$.[16] For $(CO)_4Fe{=}CH(OH)$, it is calculated to be 2.00 Å for the axial isomer and 1.96 Å for the equatorial isomer. The $M{=}C_{carb}$ distance is a bit longer in the axial isomer than in the equatorial isomer probably because the nonbonding interaction between CO and carbene is larger in the former than in the latter.

The force constant and the vibrational frequency for the $M{=}C_{carb}$ bond were calculated from the potential curve and are given in Table II. The vibrational frequency was calculated from the force constant in two approximations; the atoms and groups of atoms bonded to the metal and carbene carbon atoms are considered to completely follow or not to follow the vibration. The former approximation gives a minimum value and the latter a maximum one. The experimental vibrational frequencies $\nu(M{-}C(O))$ in $Cr(CO)_6$ and $Fe(CO)_5$ are 391–449 and 377–474 cm^{-1}, respectively.[28] The vibrational frequency $\nu(M{-}C_{carb})$ is expected

(22) Lengel, R. K.; Zare, R. N. *J. Am. Chem. Soc.* **1978**, *100*, 7495.
(23) Hirao, K.; Nakatsuji, H. *Chem. Phys. Lett.* **1981**, *79*, 292.
(24) Nagase, S.; Morokuma, K. *J. Am. Chem. Soc.* **1978**, *100*, 1661.
(25) Krüger, C.; Barnett, B. L.; Brauer, D. In "The Organic Chemistry of Iron"; von Gustorf, E. A. K., Grevels, F.-W., Fischler, I., Eds.; Academic Press: New York, 1978; Vol. 1, p 1.
(26) Davis, M. I.; Speed, C. S. *J. Organomet. Chem.* **1970**, *21*, 401.
(27) The interaction energy between $Ni(PR_3)_2$ (R = O-2-tolyl) and ethylene in $Ni(PR_3)_2C_2H_4$ is 33 kcal/mol (Tolman, C. A. *J. Am. Chem. Soc.* **1974**, *96*, 2780), and then the corresponding value in $Fe(CO)_4C_2H_4$ is expected to be smaller than this value and smaller than the interaction energy between iron and carbene calculated to be 36.8 kcal/mol (Table II).

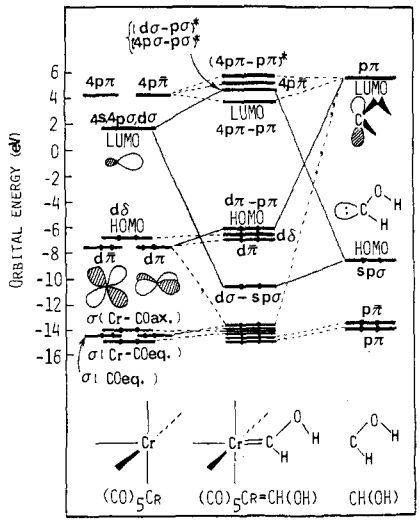

Figure 6. Correlation diagram of orbitals of $(CO)_5Cr{=}CH(OH)$ with those of the singlet fragments ($\bar{\pi}$ denotes an AO perpendicular to the π AO).

to be smaller than the ν(M–C(O)) as explained below, and the calculated frequencies given in Table II seem to be reasonable.

The results summarized in this section show that the $M{=}C_{carb}$ bonds in the Cr and Fe carbene complexes are of considerable stability and strength. The origin and the nature of this bond are further clarified with the use of the orbital correlation diagram.

Orbital Correlation Diagram

A useful way of understanding the nature and the origin of the $M{=}C_{carb}$ bond is to correlate the MO's of the metal carbene complex with the MO's of the fragments. Figure 6 shows a correlation diagram of the orbitals of $(CO)_5Cr{=}CH(OH)$ with those of the singlet fragments. In Table III, we have summarized orbital energies and coefficients of some important MO's of the complex and the fragments. As illustrated in the right-hand side of Figure 6, the HOMO of the carbene is the sp hybrid lone pair on carbon and the LUMO is the $p\pi$ orbital on carbon which is antibonding with the $p\pi$ AO on oxygen. The six valence electrons of chromium atom of the $(CO)_5Cr$ fragment occupy three d-type lone-pair MO's. The HOMO is the $d\delta$ lone pair and the next HOMO the degenerate $d\pi$, $d\bar{\pi}$ lone pairs (we denote d_{yz} and d_{xz} AO's as $d\pi$ and $d\bar{\pi}$ AO's, respectively). The LUMO is the spd hybrid σ MO extending outward at Cr and the next LUMO are the degenerate MO's composed mainly of the 4p AO's of Cr. The MO's of the complex $(CO)_5Cr{=}CH(OH)$ are correlated with the MO's of the fragments as follows. The σ bond of the $Cr{=}C_{carb}$ double bond is formed by the electron transfer interaction from the HOMO of the carbene to the LUMO of the $(CO)_5Cr$. The π bond is formed through the back-transfer of electrons from one of the degenerate $d\pi$ orbitals to the LUMO of the carbene. The $d\delta$ orbital, which is the HOMO of the $(CO)_5Cr$ fragment, has no interaction counterpart in the carbene, so that it is little affected by the complex formation. Thus, the origin of the $Cr{=}C_{carb}$ double bond is the σ transfer from carbene to Cr and the π back-transfer from Cr to carbene.

From the orbital energy of the HOMO, the first ionization potential of the Cr carbene complex is estimated to be 6.75 eV. This value may be compared with the experimental value 7.46 eV for the similar complex $(CO)_5CrC(OMe)Me$.[29]

Figure 7 shows the contour map of the σ and π bonding MO's of the Cr carbene complex. The σ MO is on the left-hand side. It shows a typical pattern of the σ bond between the Cr and C_{carb} atoms. The right-hand side is for the π MO. It also shows a beautiful pattern of the $d\pi$–$p\pi$ bond not only between the Cr and carbene carbon but also between the Cr and CO carbon.

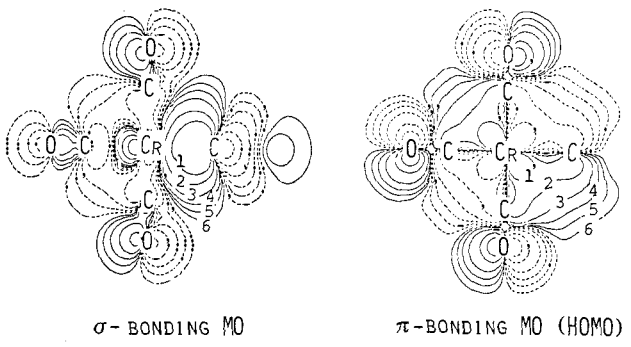

Figure 7. Contour maps of the σ and π bonding MO's of $(CO)_5Cr{=}C$-H(OH). The intersection is perpendicular to the plane of the carbene group and includes the $Cr{-}C_{carb}$ bond. Solid and broken lines correspond to the plus and minus signs in the MO's. The numbers 1–6 on contours correspond to the values (au) 0.1, 0.05, 0.02, 0.01, 0.005, 0.002, respectively.

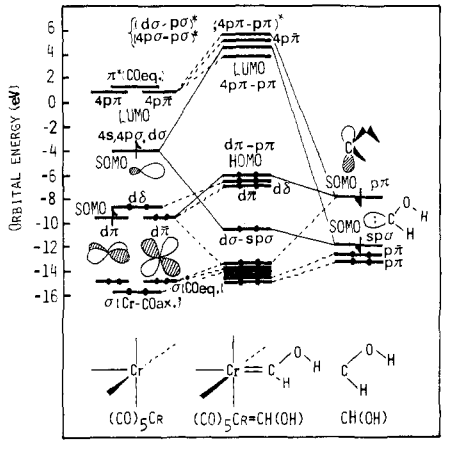

Figure 8. Correlation diagram of orbitals of $(CO)_5Cr{=}CH(OH)$ with those of the triplet fragments ($\bar{\pi}$ denotes an AO perpendicular to the π AO).

The origin of the very small rotational barrier is easily understood from the correlation diagram (Figure 6). Since the $d\pi$ level of the $(CO)_5Cr$ fragment is degenerate, it is always possible to form a new set of degenerate $d\pi'$ orbitals by an orthogonal transformation, which corresponds to rotating, without loss of energy, the original $d\pi$ orbitals around the z axis. Thus, the extent of the π back-transfer interaction between the $d\pi$ orbitals of Cr and the $p\pi$ orbital of carbene is independent of the rotational angle. The barrier to rotation is therefore determined by the secondary effects such as the interactions between nonbonded atoms, etc. so that it is of the order of the rotational barrier of the single bond.

Figure 8 shows a correlation diagram of orbitals of $(CO)_5Cr{=}CH(OH)$ with those of the *triplet* fragments. This diagram differs from Figure 6 only in the MO's of the fragments.[30] The orbital energies of the higher SOMO's, which were the LUMO's in Figure 6, become lower here because of an occupation of an electron. The bond formation from the triplet fragments is not a result of an electron transfer and back-transfer, but a result of an exchange of electrons between the σ-type SOMO's and between the π-type SOMO's of the $(CO)_5Cr$ and CH(OH) fragments.

Figure 9 shows a correlation diagram of orbitals of the axial isomer of $(CO)_4Fe{=}CH(OH)$ with those of the singlet fragments, axial $(CO)_4Fe$ and CH(OH). Table IV shows the orbital energies and coefficients of some MO's which are important in the correlation diagram. In the free $(CO)_4Fe$, eight valence electrons of iron occupy two pairs of degenerate orbitals: the lower one is the $d\pi$, $d\bar{\pi}$ lone pairs as in the $(CO)_5Cr$ of Figure 6 and the higher one (HOMO) is composed of the $d\delta$, $4p\pi$, and $4p\bar{\pi}$ AO's

(28) Adams, D. M. "Metal-Ligand and Related Vibrations"; Arnold: London, 1967.
(29) Müller, J.; Connor, J. A. *Chem. Ber.* **1969**, *102*, 1148.

(30) The MO levels of the triplet fragments do not correspond to the ionization potential because they are the solution of the open-shell RHF method.

Table IV. Orbital Energies and Coefficients of Some Important MO's of Axial $(CO)_4Fe{=}CH(OH)$ and the Fragments $(CO)_4Fe$ and CH(OH)[a]

		$(CO)_4Fe{=}CH(OH)$			$(CO)_4Fe$			CH(OH)	
		σ bonding MO	HOMO (π)	LUMO (π)	degenerate next HOMO	degenerate HOMO	LUMO ($n\sigma$)	HOMO ($n\sigma$)	LUMO (π)
ϵ_i, eV		−11.243	−4.033	3.654	−12.024	−6.656	1.853	−8.789	5.747
Fe	$3d_{x^2}$	−0.05	0.0	0.0	0.0	0.56	−0.13		
	d_{y^2}	−0.05	0.0	0.0	0.0	−0.56	−0.13		
	d_{z^2}	0.17	0.0	0.0	0.0	0.0	0.17		
	d_{xy}	0.0	−0.44	0.08	0.08	0.25	0.0		
	d_{xz}	−0.35	0.0	0.0	0.0	0.0	0.0		
	d_{yz}	0.0	0.0	−0.29	0.94	−0.05	0.0		
	4s	0.0	0.0	0.0	0.0	0.0	0.39		
	p_x	−0.02	0.0	0.0	0.0	0.0	0.0		
	p_y	0.0	0.62	−0.03	0.04	0.47	0.0		
	p_z	0.05	0.0	0.0	0.0	0.0	0.81		
C(carbene)	2s	0.39	0.0	0.0				0.58	0.0
	p_x	0.22	0.0	0.0				0.17	0.0
	p_y	0.0	0.19	0.73				0.0	0.97
	p_z	−0.58	0.0	0.0				−0.71	0.0
C(axial)	2s	−0.03	0.0	0.0	0.0	0.0	0.32		
	p_x	0.02	0.0	0.0	0.0	0.0	0.0		
	p_y	0.0	0.12	−0.34	−0.04	0.07	0.0		
	p_z	−0.03	0.0	0.0	0.0	0.0	0.11		
C(equatorial)	2s	−0.08	0.0	0.0	−0.02	−0.02	−0.17		
	p_x	−0.05	0.0	0.0	0.01	−0.09	−0.08		
	p_y	0.0	0.29	−0.11	−0.01	0.19	0.0		
	p_z	−0.02	0.0	0.0	0.0	0.01	0.16		

[a] See Figure 1 for the coordinates.

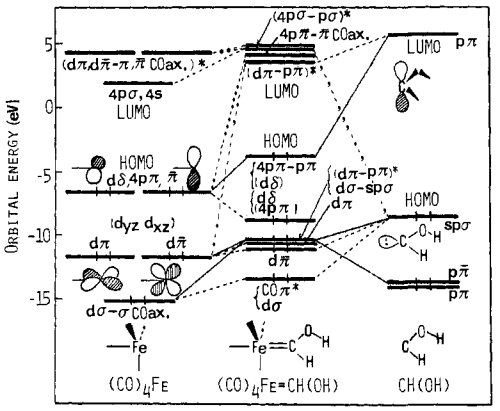

Figure 9. Correlation diagram of orbitals of the axial $(CO)_4Fe{=}C$-H(OH) with those of the axial $(CO)_4Fe$ and CH(OH) in the singlet state. ($\bar{\pi}$ denotes an AO perpendicular to the π AO).

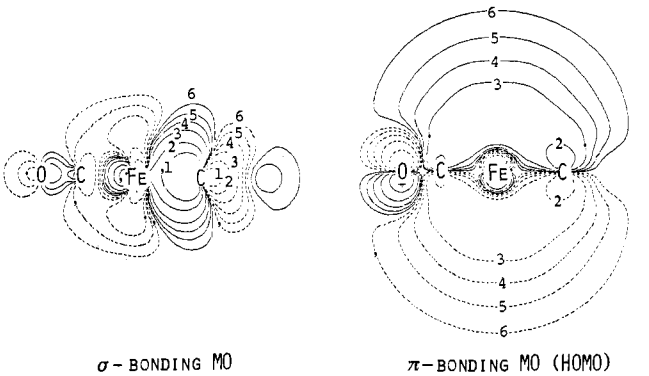

Figure 10. Contour maps of the σ and π bonding MO's of the axial $(CO)_4Fe{=}CH(OH)$. The intersection is perpendicular to the plane of the carbene group and includes the $Fe{-}C_{carb}$ bond. Solid and broken lines correspond to the plus and minus signs in the MO's. The numbers 1–6 on contours correspond to the values (au) 0.1, 0.05, 0.02, 0.01, 0.005, 0.002, respectively.

($\bar{\pi}$ denotes an AO obtained from π AO by a rotation of 90° around the σ axis). In comparison with $(CO)_5Cr$, the two more valence electrons of iron occupy 4p AO's. The LUMO is again the σ hybrid orbital, composed of the 4s and 4pσ AO's, extending out of the iron atom. The electron pair in the HOMO of the carbene attacks this LUMO of the $(CO)_4Fe$ to form the Fe–C σ bond. In Figure 10, the left-hand side gives the contour map of the resulting MO which shows a typical pattern of the σ bond between the Fe and C_{carb} atoms. By the interaction with the LUMO of the carbene, the degenerate HOMO of the $(CO)_4Fe$ splits into the 4pπ(Fe)–pπ(C) bonding π orbital and the 4p$\bar{\pi}$(Fe) lone-pair orbital. In both MO's the dδ AO of Fe mixes significantly. The second degenerate dπ, d$\bar{\pi}$ lone pairs of Fe also interact with the LUMO of the carbene, similarly as in the Cr carbene, though the interaction is much weaker here. The right-hand side of Figure 10 shows the contour map of the HOMO of the complex which shows a π bond between the diffuse 4pπ AO of the iron and the 2pπ AO's of the carbons of both carbene and axial CO. Thus, the double bond between Fe and C_{carb} in $(CO)_4Fe{=}CH(OH)$ is formed through the σ transfer and π back-transfer interactions. The π bond is the 4pπ(Fe)–pπ(C) bond, instead of the dπ-(Cr)–pπ(C) bond in $(CO)_5Cr{=}CH(OH)$. (Compare Figures 7 and 10.)

The smallness of the barrier to rotation around the Fe=C bond is explained to be due to the degeneracy of the 4pπ and 4p$\bar{\pi}$ lone pairs in the HOMO of the $(CO)_4Fe$. By a linear combination of these degenerate orbitals, a free rotation of the 4pπ AO's is represented. The rotation of the dπ AO's is also free because of the degeneracy of the next HOMO.

We note that this complete degeneracy is not necessarily a prerequisite for a small rotational barrier. Since the dπ and d$\bar{\pi}$ electrons in $(CO)_5Cr$ and $(CO)_4Fe$ and the 4pπ and 4p$\bar{\pi}$ electrons in $(CO)_4Fe$ are essentially lone pairs, they are nearly degenerate even when the symmetry is broken. For example, the rotational barrier around the $Fe{-}C_{carb}$ bond in the equatorial $(CO)_4Fe{=}$ CH(OH) is 3.6 kcal/mol, despite that the equatorial $(CO)_4Fe$ does not have an enough symmetry to have degenerate orbitals. Thus, we believe that the smallness of the rotational barrier around the $M{-}C_{carb}$ bond is common to all the Fischer-type metal carbene complexes.

Charge Distribution

A commonly accepted idea on the charge distribution in the metal carbene complexes is that the entire carbene ligand is positively polarized with the metal carbonyl part (e.g., $(CO)_5Cr$) being negative, resulting in a relatively large dipole moment (ca. 5 D).[2] Further, the carbene carbon atom is believed to be very positively charged, on the basis of the large chemical shift, e.g.,

Table V. σ and π AO Populations of the Carbene and CO Ligands in Free States, $(CO)_5Cr{=}CH(OH)$, and $(CO)_4Fe{=}CH(OH)$[a,b]

ligand		free	$(CO)_5Cr{=}CH(OH)$	$(CO)_4Fe{=}CH(OH)$ axial	$(CO)_4Fe{=}CH(OH)$ equatorial
CH(OH) carbene	σ	14.0	13.809 (−0.191)	13.810 (−0.190)	13.819 (−0.181)
	π	2.0	2.187 (+0.187)	2.188 (+0.188)	2.091 (+0.091)
CO(axial)	σ	10.0	9.830 (−0.170)	9.885 (−0.115)	9.887 (−0.113)
	π	4.0	4.338 (+0.338)	4.224 (+0.224)	4.220 (+0.220)
CO(equatorial)	σ	10.0	9.833 (−0.167)	9.813 (−0.187)	9.768 (−0.232)
	π	4.0	4.326 (+0.326)	4.326 (+0.326)	4.432 (+0.432)

[a] For equatorial CO, the average value is shown. [b] Values in parentheses show the amounts of the transfer (negative) and back-transfer (positive).

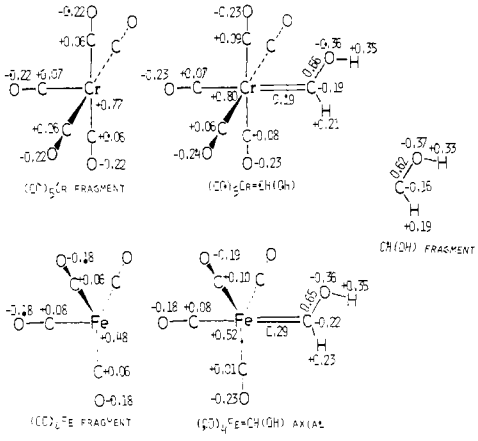

Figure 11. Net gross atomic charges in $(CO)_5Cr{=}CH(OH)$, axial $(CO)_4Fe{=}CH(OH)$, and their singlet fragments.

362.3 ppm for $(CO)_5CrC(OMe)Me$[31] and of the reactivity that the carbene carbon behaves as an electrophilic center.[2]

Figure 11 shows the calculated charge distributions of $(CO)_5Cr{=}CH(OH)$, $(CO)_4Fe{=}CH(OH)$(axial), and their fragments. Tables V and VI show the selected AO populations. Though the formal charges of Cr and Fe in these complexes are zero, the calculated gross atomic charges are large positive, +0.80 and +0.52, respectively. The carbene carbon is negatively charged −0.19 and −0.22 in the Cr and Fe carbenes, respectively. In the isolated singlet state, the carbene carbon is charged by −0.16, and so it becomes a bit more negative in the complexes. Spangler et al.[8] also reported the polarization of charge, Ni(+0.53)–C(−0.58), for the $Ni{-}C_{carb}$ bond in $(CO)_3Ni{=}CH_2$. These polarizations of charge in the M=C bonds are very natural from the electronegativity[32] of the atoms involved. As is well-known, the Fischer-type metal carbene complexes are amenable to nucleophilic attacks and the carbene carbon is the site of attack.[2] The present results show that this reactivity is not charge controlled. It is frontier controlled,[33] as will be shown below.

The sum of the charges in the CH(OH) fragment in the complex is very close to zero for both complexes, showing that the amounts of the σ transfer and π back-transfer between metal and carbene fragments are almost equal. Actually, Table V shows that the changes in the number of the σ and π electrons of the carbene by complex formation are −0.191 and +0.187, respectively, for $(CO)_5Cr{=}CH(OH)$ and −0.190 and +0.188, respectively, for $(CO)_4Fe{=}CH(OH)$. In contrast, in the CO ligands, the carbon is positively charged by ~0.07 for both complexes and the sum of the gross charges on C and O are negative by ~−0.14 for $(CO)_5Cr{=}CH(OH)$ and ~−0.10 for $(CO)_4Fe{=}CH(OH)$, because, as is well-known, the amount of the π back-transfer is larger than that of the σ transfer. For example, in $(CO)_5Cr{=}CH(OH)$,

Table VI. Valence AO Populations on the Metal Atom[a,b]

AO	$(CO)_5Cr{=}CH(OH)$ frag-ment	$(CO)_5Cr{=}CH(OH)$ com-plex	$(CO)_4Fe{=}CH(OH)$ axial frag-ment	$(CO)_4Fe{=}CH(OH)$ axial com-plex	$(CO)_4Fe{=}CH(OH)$ equatorial frag-ment	$(CO)_4Fe{=}CH(OH)$ equatorial com-plex
$3d_{x^2}$	0.18	0.19	0.65	0.88	0.19	0.16
d_{y^2}	0.18	0.20	0.65	0.91	0.22	0.35
d_{z^2}	0.08	0.20	0.08	0.17	0.02	0.32
d_{xy}	1.31	1.40	1.23	0.56	1.90	1.87
d_{xz}	1.58	1.57	1.89	1.90	1.92	1.89
d_{yz}	1.58	1.31	1.89	1.85	1.90	1.69
sum	4.91	4.87	6.39	6.27	6.15	6.28
4s	0.07	0.05	0.15	0.14	0.18	0.15
p_x	0.08	0.07	0.49	0.29	0.06	0.05
p_y	0.08	0.08	0.49	0.70	0.20	0.34
p_z	0.04	0.07	0.03	0.08	0.94	0.67
sum	0.27	0.27	1.16	1.21	1.38	1.21

[a] See Figure 1 for the coordinates. [b] In the ground state of the free atom, the population is d^5s^1 in Cr and d^6s^2 in Fe.

the amounts of the σ transfer and π back-transfer of CO are 0.170 and 0.338, respectively, for the axial CO and 0.167 and 0.326, respectively, for the equatorial CO (Table V). Thus, between the metal–carbene and metal–CO bonds, the σ bond seems to be a bit stronger in the metal–carbene bond, but the π bond is much stronger in the metal–CO bond. This is reflected in the M–C length; the M–CO distance (1.87 Å) is shorter than the $M{-}C_{carb}$ distance (~2.0 Å). Further, comparing the axial and equatorial Fe complexes, we see that the amount of π back-transfer in the equatorial isomer (+0.091) is about half of that in the axial isomer (+0.188). This is probably a reason why the axial isomer is more stable than the equatorial isomer. In both isomers of the Fe complex, the equatorial CO interacts more strongly with the iron than the axial CO.

It is to be noted that the bond population between C and O of the carbene (0.66 in $(CO)_5Cr{=}CH(OH)$, 0.65 in $(CO)_4Fe{=}CH(OH)$, and 0.62 in free CH(OH)) is median of those of the double bond (0.81 in $H_2C{=}O$) and the single bond (0.46 in $H_3C{-}OH$). The CO bond in the carbene CH(OH) therefore has a partial double bond character. This is confirmed from the existence of the cis and trans isomers with respect to the C–O bond in the carbene complexes.[3]

Table VI shows the valence AO populations on the metal atom. The positive charges of Cr (+0.86) and Fe (+0.53) are almost due to the decrease of the valence electrons. In the Cr complex, the changes due to the complex formation are seen in the increase of the $d_{z^2}(d\sigma)$ population and the decrease of the $d_{yz}(d\pi)$ population. This is a very natural result. In the Fe complex, the changes in the AO population due to the complex formation are more complex. The reorganization among the AO's seems to be important in the Fe complex. Between the Cr and Fe complexes, the most remarkable difference lies in the role of the 4p AO's. In the Cr complex, the 4s and 4p AO's are almost empty, but in the Fe complex, the 4p AO plays an important role. This was mentioned previously in the accounts of the orbital correlation diagram.

The dipole moments of $(CO)_5Cr{=}CH(OH)$ and $(CO)_4Fe{=}CH(OH)$ are calculated to be 5.28 D and 4.50 D, respectively.

(31) Farnell, L. F.; Randall, E. W.; Rosenberg, E. *J. Chem. Soc., Chem. Commun.* **1971**, 1078.
(32) Allred, A. L.; Rochow, E. G. *J. Inorg. Nucl. Chem.* **1958**, *5*, 264.
(33) Fukui, K.; Yonezawa, T.; Shingu, H. *J. Chem. Phys.* **1952**, *20*, 722. Fukui, K. "Theory of Orientation and Stereoselection"; Splinger-Verlag; Berlin, 1975.

Table VII. Analysis of the Charge of the Carbene Carbon Atom

molecule[a]	population π	σ	$\pi + \sigma$	net gross charge
$(CO)_5Cr=\overset{*}{C}H(OH)$	0.484	5.710	6.194	−0.194
$(CO)_4Fe=\overset{*}{C}H(OH)$ axial	0.486	5.732	6.218	−0.218
equatorial	0.422	5.739	6.161	−0.161
$\overset{*}{C}H(OH)$ fragment	0.321	5.837	6.158	−0.158
$H_2C=\overset{*}{C}H(OH)$	1.011	5.112	6.123	−0.123
$H_2C=\overset{*}{C}H_2$	1.000	5.519	6.519	−0.519

[a] Charge on the carbon with asterisk is analyzed.

Though these values seem to be large in comparison with 3.61 D[3] and 4.08 D[34] observed for $(CO)_5Cr=CR(OMe)$ with R = Me and Ph, respectively, this result implies that the large dipole moment actually results even if the metal carbene bond is polarized as $M^{\delta+} = C^{\delta-}$, contrary to the common idea.

The results obtained in this paper seem to indicate that the common idea that the carbene carbon of the metal carbene complexes is very positively charged is erroneous. Though we have not yet calculated the ^{13}C chemical shift from the present MO's, the two other reasons, i.e., dipole moment and reactivity, are well explained by the present results without conflicting with the fact that the carbene is negatively charged. (As for the reactivity, see the next section.)

Lastly in this section, we note another view on the charge of the carbene carbon, which helps to resolve the above conflict. In Table VII, we have shown an analysis of the charge of the carbene carbon into π and σ components. Though the net gross charges of the carbene carbons are negative, they are mainly due to the σ AO populations. The π AO populations are ~0.48 for both Cr and Fe carbene complexes. On the other hand, the π AO populations of vinyl alcohol and ethylene are 1.01 and 1.00, respectively, which may be considered as a standard "neutral" π AO population. Thus, it is true that the carbene carbons of the metal complexes are relatively electron deficient *in the π region* in contrast to the σ region, though totally they are negatively charged. It is therefore possible that a reagent may feel positive nuclear charge if it attacks from the π region of the carbene carbon atom. Nevertheless, we think that the reactivity of the carbene carbon atom is understood by the frontier control as discussed in the next section.

Reactivity—Frontier Control

It is well-known that the Fischer-type metal carbenes, as chromium and iron carbenes studied here, are readily attacked by nucleophilic reagents at the carbene carbon atom. In the preceding section, it was shown that this reactivity is not understood on the basis of the charge of the carbene carbon, because it is negatively charged. According to the frontier orbital theory of Fukui et al.,[33] the primary feature of the nucleophilic reaction is governed by the LUMO of the reactant. The site of the reaction is at the AO whose coefficient is largest in the LUMO. As seen from Tables III and IV, the $p\pi$ AO of the carbene carbon has maximum coefficient in the LUMO for both Cr carbene and Fe carbene complexes. Thus, the reactivity of the carbene complexes is understood as frontier controlled as Block, Fenske, and Casey[9] pointed out previously. In the Cr carbene, the coefficient is 0.66 and in the Fe carbene, it is 0.73. The orbital energy of the LUMO is 3.86 eV for the Cr carbene and 3.65 eV for the Fe carbene. Thus, for both orbital energy and coefficient, the carbene carbon of the Fe complex is considered to be more reactive to nucleophilic reagents than the Cr complex. In the LUMO's, the second largest coefficient is at the $4p\pi$ AO of Cr in the Cr carbene and at the $2p\pi$ AO of the axial CO in the Fe carbene. It is interesting whether such secondary reaction might exist or not for these carbene complexes. In Figure 12, the contour maps of the LUMO's of the Cr and Fe carbene complexes are shown. We see a large amplitude on the carbene carbon atom.

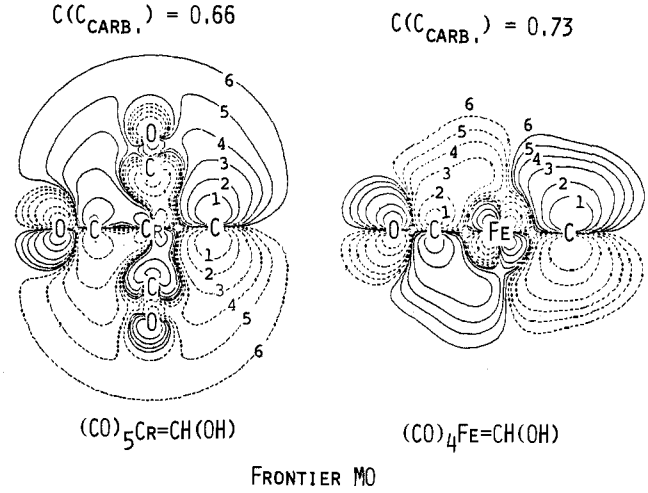

Figure 12. Contour maps of the LUMO's of $(CO)_5Cr=CH(OH)$ and axial $(CO)_4Fe=CH(OH)$. The intersection is perpendicular to the plane of the carbene group and includes the $M-C_{carb}$ bond. Solid and broken lines correspond to the plus and minus signs in the MO's. The numbers 1–6 on contours correspond to the values (**au**) 0.1, 0.05, 0.02, 0.01, 0.005, 0.002, respectively. $C(C_{carb})$ denotes the coefficient of the $p\pi$ AO of the carbene carbon atom in the LUMO.

Conclusion

In this paper, we have studied the electronic structures of the chromium and iron carbene complexes, $(CO)_5Cr=CH(OH)$ and $(CO)_4Fe=CH(OH)$, and investigated the nature of the metal carbon double bond. The $M=C_{carb}$ bond energy is calculated to be 44.4 kcal/mol for the Cr carbene and 36.8 kcal/mol for the Fe carbene. Though these values are much smaller than the C=C bond energy (120 kcal/mol) in ethylene, they still show a considerable stability of these bonds. The barrier to rotation around the $M=C_{carb}$ bond is calculated to be 0.41 kcal/mol for $Cr=C_{carb}$ and 2.9 kcal/mol for $Fe=C_{carb}$. These values are very small in comparison with the barrier, 65 kcal/mol, of the C=C bond in ethylene and are of the order of magnitude of the rotational barrier of the C–C single bond, i.e., ~3 kcal/mol. This seems to be general for the Fischer-type metal carbenes; the rotation around the $M=C_{carb}$ bond is essentially free.

For the Fe complex, the axial isomer is calculated to be more stable than the equatorial isomer by 8.1 kcal/mol. However, in the dissociation limit, the $(CO)_4Fe$ fragment is more stable in the equatorial form than in the axial one. Therefore, in the course of the dissociation of the $Fe=C_{carb}$ bond, the conformation of the $(CO)_4Fe$ will gradually change from axial to equatorial form. The bond energy, 36.8 kcal/mol, corresponds to this process.

The origin of the $M=C_{carb}$ bond is studied by the orbital correlation diagram. The σ bond is formed through an electron transfer from the σ lone-pair MO at the carbene carbon, which is a HOMO, to the vacant 4s4p3d hybrid (LUMO) extending out of the metal. The π bond is formed by the back-transfer of electrons form the degenerate $d\pi$ lone-pair MO's of $(CO)_5Cr$ or from the degenerate $4p\pi$ lone-pair MO's of $(CO)_4Fe$ to the vacant $p\pi$ MO (LUMO) of the carbene. Thus, the π bond is $d\pi-p\pi$ type in $Cr=C_{carb}$ and $4p\pi-p\pi$ type in $Fe=C_{carb}$. The amounts of the σ transfer and the π back-transfer are almost the same, in contrast to the interaction between the metal and CO, where the π back-transfer is larger than the σ transfer. The smallness of the rotational barrier around the $M=C_{carb}$ bond is understood from the degeneracy (or near degeneracy) of the π-type lone pairs in the $M(CO)_n$ fragment ($d\pi$-type lone pairs in the $(CO)_5Cr$ and $4p\pi$-type lone pairs in the $(CO)_4Fe$). The rotation of the $d\pi$ and $4p\pi$ orbitals is expressed by a linear combination (orthogonal transformation) of these degenerate orbitals (any linear combination of degenerate orbitals affects nothing on the energy and the electronic structure of the fragment molecule).

(34) Fischer, E. O.; Maasböl, A. *Chem. Ber.* **1967**, *100*, 2445.

The polarization of charge in the M=C_{carb} bond is calculated to be Cr(+0.80)-C(-0.19) and Fe(+0.52)-C(-0.22) for the Cr and Fe carbenes, respectively (values in parentheses show the gross atomic charge), though the electron is relatively deficient in the π region of the carbene carbon atom. Spangler et al.[8] also reported the gross charge Ni(+0.53)-C(-0.58) for $(CO)_3Ni{=}CH_2$. The carbene carbon is calculated to be negatively charged, in contradiction with the common idea based on the NMR ^{13}C chemical shift, large dipole moment, and reactivity (nucleophilic attack on carbene carbon). Though we have not yet calculated the ^{13}C chemical shift from the present MO's, the other two facts are well explained by the present calculations. The dipole moments of the complexes are calculated to be large and the reactivity of the complexes is not charge controlled but frontier controlled. The LUMO's of the complexes have large coefficient at the pπ AO of the carbene carbon atom. Between the Cr and Fe complexes, the Fe complex seems to be more reactive than the Cr complex from both the magnitudes of the MO coefficient and the orbital energy of the LUMO.

Acknowledgment. For the SCF calculations, we have used a slightly modified version of the HONDOG program due originally to King, Dupuis, and Rys whom the authors acknowledge. Calculations were carried out with the M-200 computers at the Institute for Molecular Science and the Data Processing Center of Kyoto University. This work was supported in part by a Grant-in-Aid for Scientific Research from the Japanese Ministry of Education, Science, and Culture.

Registry No. $(CO)_5Cr{=}CH(OH)$, 83998-88-3; *eq*-$(CO)_4Fe{=}CH(OH)$, 83998-89-4; *ax*-$(CO)_4Fe{=}CH(OH)$, 84026-47-1.

Covalent Bonding in *trans*-Tetraamminedinitronickel(II) Studied by X-ray Diffraction at 110 K

B. N. Figgis,* P. A. Reynolds, and S. Wright

Contribution from the School of Chemistry, University of Western Australia, Nedlands, Australia 6009. *Received April 2, 1982*

Abstract: The electron distribution of *trans*-tetraamminedinitronickel(II), $Ni(NH_3)_4(NO_2)_2$, has been studied at 110 K by single-crystal X-ray diffractometry. The data were analyzed by conventional least-squares methods and also by use of a model in which chemically reasonable appropriate s, p, and d hybrids were refined on all atoms. This gave R = 1.7%, R_w = 3.1% with $((\sin\theta)/\lambda)_{max}$ = 8.5 nm^{-1}. The model shows a substantial (0.38 (8) electron) σ donation of electrons from each nitrite to nickel, with no significant π contribution. The ammonia molecules each donate 0.11 (6) σ electron, which is, as expected, less than that from the nitrite ions. The valence density around the nickel is mainly 3d-like as expected (3d = 7.6 (1)), but there is a substantial 4p component (4p = 1.61 (2)). This gives a net charge on nickel of +0.8 (1). The aspherical distribution of this 3d density around the nickel atom is $3d_{xy}^{1.28(7)}3d_{yz}^{1.80(6)}3d_{xz}^{1.31(6)}3d_{z^2}^{1.36(8)}3d_{x^2-y^2}^{1.84(7)}$. This is the result expected from ligand-field theory if one takes into account the effects of covalence, except for an anomalously low d_{xz} population. The 4p electron density around the nickel atom is of orthorhombic rather than the expected tetragonal symmetry. The residual electron density also shows a further small diffuse component around the nickel atom not of 4s or 4p symmetry and features in the nitrite N-O bonds probably associated with overlap density.

The determination of both the electron density by X-ray diffraction and of spin density by polarized neutron diffraction in a single simple transition-metal complex should provide a stringent test of current theories of the electronic structure of such molecules. This is because the theories largely have been constructed to account for energetic (spectroscopic) observations not spatial (diffraction) ones. Although the effects of covalence are small in both experiments, they can be determined sufficiently well to provide new information of chemical interest. Examples are (phthalocyaninato)manganese(II)[1] and tricesium tetrachlorocobaltate(II) chloride[2] for spin densities and chromium hexacarbonyl,[3] iron pyrites,[4] and hexaamminecobalt(III) hexacyanochromate(III)[5] for charge densities.

Crystals of compounds suitable for both experiments must have a simple crystal structure, a substantial magnetic moment at 4.2 K, contain no elements highly absorbing for either X-rays or thermal neutrons, and suffer little extinction or anharmonicity in thermal motion. Crystals of *trans*-tetraamminedinitronickel(II), $Ni(NH_3)_4(NO_2)_2$, not only satisfy these restrictions, but the molecule is chemically interesting in that the nitrite anion, being high in the spectrochemical series, is expected to exert a substantial covalent effect.

Preliminary X-ray diffraction,[6,7] magnetochemical,[7,8] spectroscopic,[7] and neutron diffraction[9] experiments on this compound reveal no untoward features, such as structural or magnetic phase changes, or excessive extinction, although twinning is common. The present publication is devoted to an analysis of the X-ray diffraction data. Subsequent publications will deal with our polarized neutron data[10] and ab initio theoretical calculations.[11]

It is usual in charge-density studies to discuss the results using Fourier maps, showing the difference between the observed density and that of a suitable reference state. More recently, in connection with transition-metal complexes, it has become the practice to employ least-squares fitting of 3d electron populations on the metal

(1) Figgis, B. N.; Forsyth, J. B.; Mason, R.; Williams, G. A. *J. Chem. Soc.* **1981**, 1837-1845.
(2) (a) Figgis, B. N.; Reynolds, P. A.; Williams, G. A. *J. Chem. Soc., Dalton Trans.* **1980**, 2339-2347. (b) Chandler, G. S.; Figgis, B. N.; Phillips, R. A.; Reynolds, P. A., Mason, R.; Williams, G. A. *Proc. R. Soc. Lond, Ser. A.*, in press.
(3) Rees, B.; Mitschler, A. *J. Am. Chem. Soc.* **1976**, *98*, 7918-1924.
(4) Stevens, E. D.; Delucia, M. L.; Coppens, P. *Inorg. Chem.* **1980**, *19*, 813-820.
(5) Iwata, M. *Acta. Crystallogr., Sect. B* **1977**, *B33*, 59-69.
(6) Porai-Koshits, M. A.; Dikareva, L. M. *Sov. Phys. Crystallogr. (Engl. Transl.)* **1960**, *4*, 611-616.
(7) Figgis, B. N.; Reynolds, P. A.; White, A. H.; Williams, G. A.; Wright, S. *J. Chem. Soc., Dalton Trans.* **1981**, 997-1003.
(8) Figgis, B. N.; Kennedy, B. J.; Murray, K. S.; Reynolds, P. A.; Wright, S. *Aust. J. Chem.* **1982**, *35*, 1807-1813.
(9) Figgis, B. N.; Reynolds, P. A.; Williams, G. A.; Lehner, N. *Aust. J. Chem.* **1981**, *34*, 993-999.
(10) Figgis, B. N.; Mason, R.; Reynolds, P. A. *J. Am. Chem. Soc.* **1982**, *104* (following paper in this issue).
(11) Chandler, G. S.; Phillips, R. A., unpublished data.

0002-7863/83/1505-0434$01.50/0